ingegneria sismica
International Journal of Earthquake Engineering
Anno XLIII - Num. 2 - 2026

# Application and algorithm optimization of smart sensors in electromechanical systems

*Zhangwei Lei*[1,*]

[1] Mechanical and Electrical Engineering Department, Yuncheng University, Yuncheng 044000, Shanxi, China

**SUMMARY:** *As a cutting-edge technology, smart sensor technology provides a brand new solution for monitoring, controlling and optimizing electromechanical systems with its high precision, high sensitivity and multifunctionality. Based on the background of the application of smart sensor technology in electromechanical systems, this paper first analyzes the non-stationary signals in electromechanical systems using wavelet transform, then proposes the method of extracting the feature information of electromechanical vibration signals, and then applies the SVM parameters based on PSO to analyze the real-time key parameters of motors, and then makes early warning on the possible fault state through the running state of motors, so as to realize the monitoring of the motor's running state. Finally, the method of this paper is applied to test the electromechanical system, and the results show that the electromechanical system fault identification model can make real-time state determination of the motor running state, which helps to carry out non-stop detection and predictive maintenance of the on-line running electromechanical in the production line.*

***KEYWORDS:*** *wavelet transform; PSO; intelligent sensor; electromechanical system*

# 1 Introduction

With the continuous progress of science and technology and the rapid development of intelligent technology, intelligent sensors play an increasingly important role in electromechanical systems [1, 2]. These sensors can not only sense and collect environmental information, but also realize real-time monitoring and control of the system through intelligent data processing and communication functions [3, 4].

Sensing technology is a key technological field, the core of which lies in sensing physical or chemical quantities in the environment by sensing them and converting them into measurable signals [5, 6]. Traditional sensing technology mainly focuses on the accurate collection of data, but with the development of science and technology, smart sensing technology is gradually emerging [7, 8]. The uniqueness of smart sensing technology relative to traditional sensing technology is that it integrates advanced information technology, which makes the sensors have a higher level of intelligent capability, with adaptive, communication capability, data processing capability and energy consumption optimization [9-12]. The development and application of smart sensors will bring more efficient and intelligent solutions to various industries, and promote scientific and technological progress and social development [13, 14]. Smart sensors play a crucial role in electromechanical systems [15]. First, they can sense environmental

*leizhangwei@ycu.edu.cn
https://doi.org/10.65102/is20261002
Published: 30 April, 2026

information in real time and provide real-time data support for the system, thus realizing automation and intelligent control of the system [16, 17]. Second, the high-precision and multi-functional characteristics of smart sensors can effectively improve the performance and efficiency of the system and reduce energy consumption and resource waste [18, 19]. In addition, smart sensors are able to provide decision support through data analysis and prediction, optimize the system operation mode, and achieve more intelligent operation management [20, 21].

Aderibigbe, A.O. et al. examined the opportunities and challenges posed by advanced sensor technologies including integration complexity and development of regulatory frameworks and emphasized on adaptable and scalable sensor technologies, the results help to understand the current status and future outlook of sensing technologies for electro-mechanical systems, and provide strategic recommendations for practitioners [22]. Moon, J., and Leeb, S.B. proposed wireless sensors for electromechanical systems, from which data can be used to correlate electrical and mechanical data to differentiate between various pathologies in a machine and its mechanical installation, and fused data from multiple sensors to create a coordinated image of a machine's operation on a self-powered platform [23]. Wang,S. et al. proposed the integrated measurement method with sensing head, which incorporates the equipartitioned characteristics of the mechanical structure as part of the sensor, i.e., the self-sensing system, revealing the method to be a practical self-sensing technology with significant size reduction and intelligent control advantages in the industry [24]. Nazir, S., and Kwon, O.S. described the application of microelectromechanical systems (MEMS) based sensors in manufacturing industry, pointed out that MEMS is characterized by small size, low energy consumption, high performance, etc., and outlined the development of MEMS sensors in terms of sensing mechanisms, especially in the healthcare industry, and the advantages of its application [25]. Esashi, M. emphasized that microsensors implemented by microelectromechanical systems (MEMS) technology play a key role as input devices to the system and reviewed surface acoustic wave wireless pressure sensors, angular velocity sensors, and chemical sensors, medical sensors, etc [26]. Faudzi,A.A.M. et al. reviewed the current status of microelectromechanical systems (MEMS) applications in robotics and industry, indicating that MEMS are widely used as sensors in various applications, with tremendous advances in size reduction, reliability improvement, versatility, customized design and power consumption [27]. Zhou,G. designed a fault diagnosis and monitoring system for electromechanical equipment based on group intelligent sensing technology, which is designed so that users, manufacturers and other parties of electromechanical equipment can break through the limitations of time and space, and all of them are able to communicate in real time about the problems that occur in the equipment, which promotes the more efficient automation and intelligent maintenance of electromechanical equipment [28].

Based on the basic principles and characteristics of smart sensors, the article summarizes the applications of smart sensors in manufacturing, transportation, energy, agriculture and other fields. Then the wavelet transform is proposed to analyze the non-stationary signal of electromechanical system to extract the feature information of electromechanical system in time-frequency domain and input it into Support Vector Machine (SVM) for training. A fault identification model of electromechanical system based on feature extraction and particle swarm algorithm (PSO) optimized support vector machine (SVM) is also designed. Finally, the acquisition and analysis of vibration signals, which can intuitively and quickly reflect the operating characteristics of electromechanical systems, are taken as an example to experiment the method proposed in this paper.

# 2 Application of smart sensor technology in electromechanical systems

## 2.1 Basic Principles and Characteristics of Smart Sensors

Smart sensor is a set of sensing, processing and communication in one of the advanced sensing technology, its application in electromechanical systems has been widely concerned and attention. Smart sensor is through the process technology means the sensor and microprocessor are closely integrated, the sensor's sensitive components and its signal conditioning circuit and microprocessor integrated in a chip on the new processor, which is not only able to realize the functions of the traditional sensors, but also make full use of the microprocessor's computing and storage capabilities. Smart sensors collect, process and transmit a large amount of data information in real time through the internally integrated sensing elements, signal processing circuits and communication interfaces, etc., and autonomously carry out intelligent analysis and decision-making, so as to realize the precise monitoring and control of electromechanical systems [29]. The basic principle of smart sensors is to convert physical quantities or environmental information into quantifiable electrical signals by sensing them. Different physical quantities use sensor elements with different working principles, such as resistance, capacitance, inductance, piezoelectric effect, photoelectric effect, etc. When the physical quantity changes, the sensor element produces corresponding changes, which are converted into readable electrical signals through signal processing circuits. Compared with traditional sensors, smart sensors have the following advantages.

First, smart sensors have integrated signal processing circuits and algorithms inside, with certain data processing and analyzing capabilities, which can provide richer and more valuable information. Secondly, smart sensors have communication interfaces, which can interact and interconnect data with other sensors, control systems or networks to realize information sharing, collaborative control and remote monitoring and other functions. Third, smart sensors have a certain degree of intelligence, can be based on internal algorithms and models for data analysis and decision-making, to achieve autonomous operation and control. Fourth, smart sensors can integrate a variety of sensing elements to realize simultaneous sensing and measurement of multiple physical quantities, with a wider range of application areas and functions. Fifth, smart sensors have higher sensitivity, flexibility, embeddedness and resistance to electromagnetic interference. Sixth, smart sensors also have fault detection and self-diagnostic functions, can monitor their own state and provide timely alarms or fault information to improve the reliability and stability of the system. Seventh, smart sensors usually tend to be designed with smaller size and lower power consumption to fit various application scenarios and easy integration, while traditional sensors may be more concerned about data accuracy and reliability, with relatively larger size and power consumption.

## 2.2 Application cases of smart sensors in electromechanical systems

In the manufacturing sector, smart sensors are widely used for equipment monitoring and predictive maintenance. For example, smart sensors can monitor the operating status, vibration and temperature of machines and other parameters in real time, and through data analysis and pattern recognition, predict equipment failures in a timely manner and provide accurate predictive maintenance recommendations, and this application can greatly reduce equipment failures and downtime, and improve production efficiency and product quality. Smart sensors also play an important role in the field of transportation. For example, smart sensors used in traffic flow monitoring can sense the number and flow rate of road vehicles in real time, and through data analysis and processing, they can accurately assess the traffic situation and provide real-time traffic decision support for traffic management departments. In addition, smart sensors can also be used for intelligent driving and automatic parking of vehicles, etc., to improve traffic safety and transportation efficiency. In the field of energy, smart sensors are applied to the monitoring and optimization of energy consumption. For example, smart energy meters can monitor power consumption in real time and provide accurate power consumption information and energy management suggestions to help users optimize energy use and reduce energy waste. Smart sensors can also be used to monitor and control renewable energy sources, such as solar and wind power, to improve the efficiency of energy utilization. In the field of agriculture, smart sensors can be used for monitoring soil moisture, meteorological conditions and crop growth status By installing a network of smart sensors, the environmental parameters of the farmland can be monitored in real time and the data can be transmitted to a central control system to help farmers make precise irrigation decisions and crop management strategies, and this kind of intelligent agricultural management can improve the yield and quality of agricultural products, while saving water resources and the pesticide use.

# 3 Electromechanical system fault identification model design

## 3.1 Wavelet transform

Set $\psi(t) \in L^2(R)$ if satisfied:

$$\int_{-\infty}^{\infty} \frac{\bar{\psi}(\omega)}{|\omega|} d\omega < \infty \tag{1}$$

Then $\psi(t)$ is said to be a fundamental wavelet and wavelet mother function. Where $\bar{\psi}(\omega)$ is the Fourier transform of the function $\psi(t)$. Eq. can also be referred to as the admissibility condition. Let:

$$\psi_{a,b}(t) = |a|^{-\frac{1}{2}} \psi\left(\frac{t-b}{a}\right) \tag{2}$$

where $b \in R$ and $a \in R - \{0\}$, Eq. is called the fundamental or mother wavelet. $\psi(t)$ depends on the continuous wavelet generated by $a,b$, where Eq. $a$ is called the scale factor, which can change the shape of the continuous wavelet. $b$ is the displacement factor, which can change the displacement of the continuous wavelet. The continuous wavelet $\psi_{a,b}(t)$ possesses localization both in the time domain and in the frequency domain, and its effect is equivalent to the window function in the short-time Fourier transform. Thus the wavelet transform of the function $f(t)$ is:

$$W_f(a,b) = \langle f, \psi_{a,b} \rangle = |a|^{-\frac{1}{2}} \int_{-\infty}^{\infty} f(t) \bar{\psi}\left(\frac{t-b}{a}\right) dt \tag{3}$$

where $\bar{\psi}(t)$ is the complex conjugate of the function $\psi(t)$ by the admissibility condition:

$$\int_{-\infty}^{\infty} \psi(t) dt = 0 \tag{4}$$

The inverse transformation of $W_f(a,b)$ is:

$$f(t) = \frac{1}{c_\psi}\iint_R W_f(a,b)\psi_{a,b}(t)\frac{dadb}{a^2} \tag{5}$$

In the formula:

$$C_\psi = \int_{-\infty}^{\infty}\frac{|\overline{\psi}(\omega)|^2}{|\omega|}d\omega < \infty \tag{6}$$

If the corresponding wavelet coefficients are computed based on all possible scaling factors and their translation parameters, a large amount of useless data will be generated. If both the scaling factor and the translation parameter are chosen to be multiples of $2^j$ ($j > 0$ and integer), the amount of data to be analyzed can be greatly reduced [30]. The double scale wavelet transform is a type of discrete wavelet transform, and it is the wavelet transform that utilizes this scaling factor and translation parameter.

The discrete wavelet transform is the transformation of the "original signal $S$" into "wavelet coefficients $W$", where $W = [W_a, W_d]$, the original signal is the approximation coefficients $W_a$ and the detail coefficients $W_d$. The wavelet decomposition is the product of the components of the wavelet coefficients $W$ and the basis function.

The components of the original signal mapped onto the wavelet basis are defined as the discrete wavelet positive transform. Let $n = 1, \cdots, M$, $s(n)$ be the original signal and the wavelet coefficients $w_J$ be:

$$w_J = [w_{aJ}, w_{dJ}, \cdots, w_{d1}] \tag{7}$$

In the formula:

$$w_{aJ} = \langle s(n) \cdot A_J(n) \rangle \tag{8}$$

$$w_{dj} = \langle s(n) \cdot D_j(n) \rangle \tag{9}$$

where $j = J, \cdots, 1$.

The discrete wavelet inverse transform is a decomposition of all wavelets to synthesize the original signal. The transform equation is:

$$s(n) = a_j(n) + \sum_{j=1}^{J} d_i(n) = w_{aj}A_j(n) + \sum_{j=1}^{J} w_{dj}D_j(n) \tag{10}$$

where $A_y(n), D_j(n)$ is the wavelet basis function.

From the implementation of wavelet decomposition, the original signal is passed through a low-pass filter to get the approximate coefficients, and through a high-pass filter to get the detailed coefficients. The decomposition is then repeated for the low frequency part according to the decomposition level of the signal frequency. According to the wavelet decomposition of the signal, and then focus on the spectral analysis of the detail signal, the fault frequency can be effectively extracted.

## 3.2 Electromechanical vibration signal feature information extraction

### 3.2.1 Time and frequency domain feature information extraction parameters

The time-domain parameters mainly include 10 indexes such as amplitude, variance, rms, rms, skewness, cragness, waveform factor, etc. of the pallet vibration signal. Among them, quantitative time-domain features such as amplitude and rms are more sensitive to the operating state of the equipment, and can effectively identify weak fault characteristics. The disadvantage is that it is highly susceptible to the influence of the operating parameters of the equipment. On the other hand, dimensionless time-domain features such as waveform index, peak index, etc. are not easily affected by the operating parameters of the equipment, which reflect the shape of the probability density function of the vibration signal, so the combination of quantitative and dimensionless physical parameters can characterize the characteristics of the vibration signal of the carrier wheel in a more comprehensive way.

When the failure of the equipment occurs, the energy of a certain frequency band of the collected signal will produce a large change, while the energy of other signal bands will change less. This indicates that, in the support wheel vibration mode change, the frequency domain characteristics of the vibration signal will also change, such as a certain frequency component of the energy appears to increase significantly. Since frequency characteristics such as mean square frequency, median frequency, root mean square frequency, frequency variance, etc. can describe the degree of spectral dispersion and frequency energy changes, therefore, the frequency characteristics can characterize the support wheel vibration mode changes. Among them, the formulae for calculating the characteristic parameters in the time and frequency domains are shown in Table 1.

*Table 1: The time domain and frequency domain feature calculation formula*

| Feature Name | Computational Formula | Feature Name | Computational Formula |
|---|---|---|---|
| Mean | $F_1 = \frac{1}{N}\sum_{k=1}^{N} x(n)$ | Frequency Mean | $F_{11} = \frac{\sum_{k=1}^{k} s(k)}{K}$ |
| Standard Deviation | $F_2 = \sqrt{\frac{1}{N-1}\sum_{i=1}^{N}\left(x(n)-F_1\right)^2}$ | Frequency Center Value | $F_{12} = \frac{\sum_{k=1}^{k} f_k s(k)}{\sum_{k=1}^{k} s(k)}$ |
| Mean Square | $F_s = \frac{1}{N}\sqrt{\sum_{n=1}^{N} x^2(n)}$ | Frequency Mean Square Root | $F_{13} = \sqrt{\frac{\sum_{k=1}^{k} f_k^2 s(k)}{\sum_{k=1}^{k} s(k)}}$ |
| Peak | $F_4 = \max\lvert x(n)\rvert$ | Frequency Deviation | $F_{14} = \sqrt{\frac{\sum_{k=1}^{k}(f_k - F_{12})^2 s(k)}{K}}$ |
| Rake | $F_5 = \frac{N}{(N-1)(N-2)}\sum_{n=1}^{N}(\frac{x(n)-F_1}{F_2})^3$ | Mean Frequency Value | $F_{15} = \sqrt{\frac{\sum_{k=1}^{k} f_k^4 s(k)}{\sum_{k=1}^{k} f_k^2 s(k)}}$ |
| Sheer | $F_6 = \frac{1/N\sum_{s=1}^{N}\left(\lvert x_s\rvert - F_s\right)}{F_s^4}$ | Stability Factor | $F_{16} = \sqrt{\frac{\sum_{k=1}^{k} f_k^2 s(k)}{\sum_{k=1}^{k} s(k)\, f_k^4 s(k)}}$ |
| Peak Coefficient | $F_\gamma = \frac{\max\lvert x(n)\rvert}{\sqrt{\frac{1}{N}\sum_{i=1}^{N} x(n)^2}}$ | Variation Coefficient | $F_{17} = \frac{F_{14}}{F_{11}}$ |
| Clearance Coefficient | $F_8 = \frac{\max\lvert x(n)\rvert}{\left(\frac{1}{N}\sum_{i=1}^{N}\sqrt{\lvert x(n)\rvert}\right)^2}$ | Frequency Range | $F_{18} = \frac{\sum_{k=1}^{K}(f_k - F_{11})^3 s(k)}{KF_{14}^3}$ |
| Form Factor | $F_9 = \frac{\sqrt{\frac{1}{N}\sum_{i=1}^{N} x(n)^2}}{\frac{1}{N}\sum_{i=1}^{N}\lvert x(n)\rvert}$ | Frequency Sheer | $F_{19} = \frac{\sum_{k=1}^{K}(f_k - F_{15})^4 s(k)}{KF_6^4}$ |
| Impact Factor | $F_{10} = \frac{\max\lvert x(n)\rvert}{\frac{1}{N}\sum_{i=1}^{N} x(n)}$ | The Ratio Of The Average Square Root Of The Frequency Domain | $F_{20} = \frac{\sum_{i=1}^{K}(f_i - F_{15})^2 s(k)}{K\sqrt{F_{15}}}$ |

where $x(n)$ is the sequence of collected data and $N$ is the sampling length. $s(k)$ is the sequence of spectral lines of $x(n)$ and $f_k$ is the frequency value of $x(n)$ at point $k$. $K$ is each frequency spectral line.

### 3.2.2 Time-frequency domain feature information extraction parameters

Frequency domain signal processing methods such as empirical modal decomposition, wavelet analysis, etc. have been widely researched and used in recent years, and compared with the time domain and frequency domain feature processing methods, they have a better processing effect for the non-smooth signal containing strong background noise such as the vibration signal of the support wheel. Therefore, by calculating the energy of the signal components in the frequency band sensitive to signal faults, the faults of the equipment can be recognized effectively.

We have adopted the CEEMD method with adaptive capability for time-frequency domain feature parameter extraction. When using CEEMD for feature extraction, firstly, a finite number of eigenmode functions can be obtained by decomposing the signal layer by layer [31]. The specific process of the feature extraction method for the vibration signal of the pallet is as follows:

Step 1: CEEMD decomposition of the original signal. Firstly, the original signal is denoised by mean value, and then the denoised signal is decomposed by CEEMD method, which can get a series of IMF components. And FFT transform is applied to each IMF component.

Step 2: According to the pallet vibration model studied in Chapter 3, the IMF components containing the frequency components of cylinder harmonics (KH), and pallet harmonics (RH) are selected.

Step 3: Calculate the sensitive component energy, and the expression of the energy calculation formula for the IMF component is as follows:

$$E_i = \sum_{j=1}^{N} | a_i(t) |^2 \tag{11}$$

Taking the sensitive component energy as the feature parameter, the following time-frequency domain feature set can be constructed:

$$D = \{E_1, E_2 .........E_n\} \tag{12}$$

In order to avoid the influence of large values on small value features in the set of time-frequency features, it is necessary to normalize the set $D$, and the normalization formula is as follows:

$$EG_i = \frac{E_i}{\sqrt{\sum_{i=1}^{n} |E_i|^2}} \tag{13}$$

Ultimately, the resulting feature set can be represented as:

$$DE = \left\{EG_1, EG_1 ......EG_n\right\} \tag{14}$$

## 3.3 Optimized SVM parameter-based fault diagnosis model

### 3.3.1 SVM Fundamentals

Support vector machine is currently one of the mainstream machine learning methods. Since the original data of transformer sound signal is less and the accumulation of public dataset is more difficult at present, SVM, which can solve the classification problem under small samples, is chosen to have advantages over neural network algorithms, such as strong generalization ability and no local minima problem.

The basic idea of Support Vector Machine is to divide the data into 2 groups, one as a test set and the other as a validation set. The support vector machine is shown in Figure 1. The input data samples with different categories are separated by finding an optimal hyperplane as shown in the figure, the hyperplane formula can be expressed as:

$$\omega^T X + b = 0 \tag{15}$$

where $\omega$ is the determining hyperplane normal vector. $b$ is the displacement. $X$ is the acoustic signal training sample.

The problem of maximizing the distance between any point on the hyperplane and the two edge hyperplanes on either side is transformed into a convex quadratic programming problem by dividing the expression:

$$Min = \frac{1}{2}\|\omega\|^2 + C\sum_{i=1}^{N}\xi_i \tag{16}$$

where $C$ is the penalty factor. $\xi_i$ is the relaxation factor. The model generalization ability is improved by introducing the relaxation factor $\xi_i$. The selection of the penalty factor $C$ and the kernel function $g$ has a great influence on the classification accuracy of SVM, and this paper adopts the particle swarm algorithm to find the optimization of these 2 parameters.

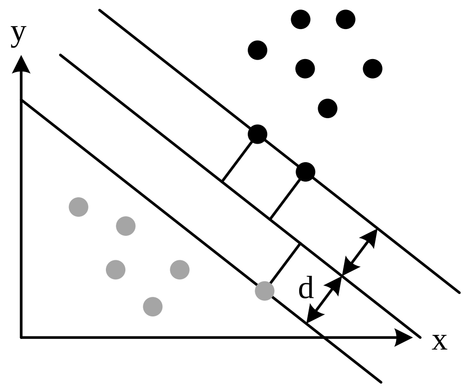


*Figure 1: Illustration of the support vector machine*

### 3.3.2 Particle Swarm Optimization Algorithm

Particle Swarm Optimization Algorithm (PSO) is an intelligent algorithm with high solution accuracy that searches for the optimal solution in the whole environment by updating the position and velocity strategies of the particles. By simulating the foraging behavior of birds in nature, by simulating the search for the area around the nearest bird to the food. The birds are compared to particles and their positions are determined by their velocities, and the optimal solution is obtained by iterating through a randomized particle swarm.

The particle swarm algorithm velocity update formula and position update formula are:

$$v_{id}^{k+1} = \omega v_{id}^{k} + c_1 r_1 (p_{id,pbect}^{k} - x_{id}^{k}) + c_2 r_2 (p_{d,gbect}^{k} - x_{id}^{k}) \tag{17}$$

$$x_{id}^{k+1} = x_{id}^{k} + v_{id}^{k+1} \tag{18}$$

where $v_{id}^{k}$ is the velocity vector of particle $i$ in the $d$ th dimension in the $k$ th iteration. $x_{id}^{k}$ is the $d$ -dimensional position vector of particle $i$ in the $k$ th iteration. $\omega$ is the inertia weight, generally taken as 0.9. $r_1, r_2$ are random numbers in the interval [0, 1]. $c_1$ is the individual learning factor. $c_2$ is the group learning factor, usually taken as $c_1 = c_2 = 2$.

### 3.3.3 PSO-based SVM parameter optimization

SVM parameters are usually optimized using cross-validation methods. The core concept is to divide the dataset into training set and validation set, and then train and evaluate the model performance under different parameter combinations to find the best parameter combination. The method first trains the classifier with the training set and then tests the trained model with the validation set to obtain the classification accuracy as the performance evaluation index of the classifier. However, the method has high time complexity and long computation time. For this reason, the article uses the particle swarm optimization (PSO) algorithm to find the optimal parameters of $g$ and $C$. The optimization of the parameters is achieved by constantly updating the position and velocity of the particles, and update iterations are performed to find the optimal $g$ and $C$ values quickly.The principle of PSO-SVM is shown in Fig. 2.

The PSO-based SVM parameter optimization process is as follows.

(1) According to the signal processing steps in the previous section, the acoustic signal eigenvalues are extracted to get the transformer core loosening data sample set, and the sample set is normalized. The SVM model is constructed by extracting 2096 of them as the test set and the remaining 80% as the training set.

(2) Initialize the population parameters, set the population size $n = 50$ with the maximum number of iterations $N = 100$. Calculate the fitness of the particles in each iteration, take the fusion feature values extracted from the training set of sound patterns as input data, and select the accuracy value of the SVM prediction results as the fitness function of the particle population. The highest ground particle among them is selected as the global optimal solution.

(3) Update the position and velocity of each individual particle according to whether the global optimal solution and the positions and velocities of other individual particles satisfy the requirements of accuracy and number of iterations.

(4) Repeat the execution to determine the optimal solution based on the position and velocity update of each individual particle, and update the position and velocity of each example based on the new optimal solution until the condition is satisfied, and finally output the optimal parameter combination $g$ and $C$.

(5) Finally, the optimal parameters are substituted back to the SVM model and the final optimized SVM model is obtained by training and validating it using the voiceprint data training set [32].

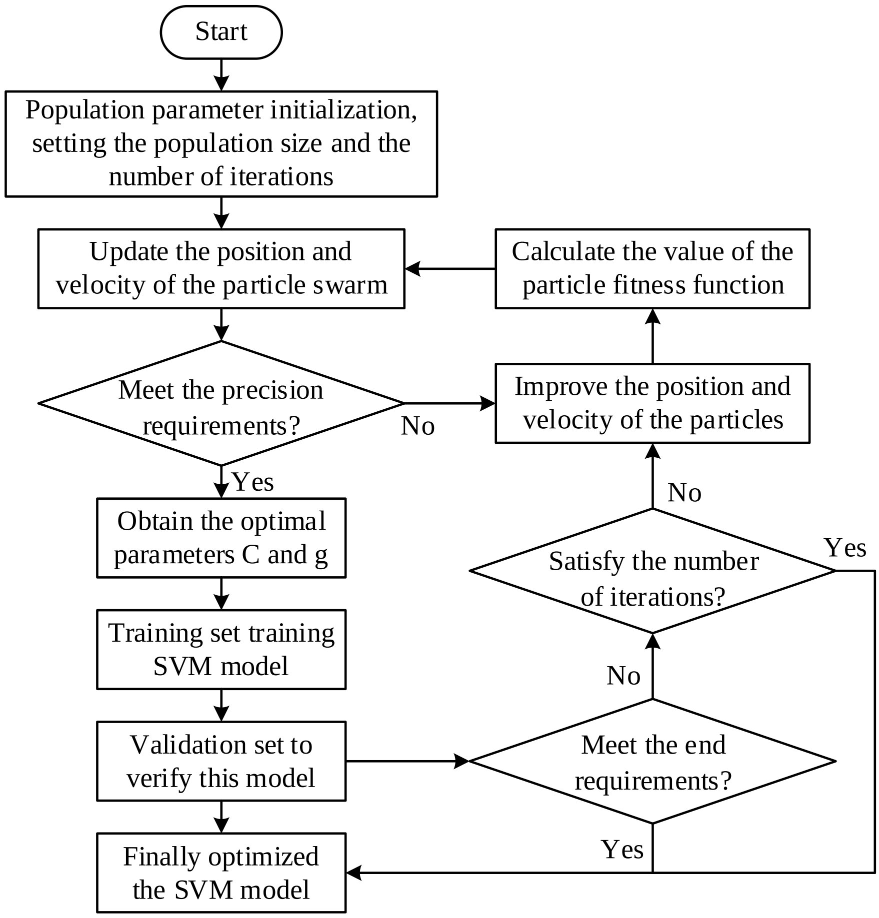


*Figure 2: Principle of PSO-SVM*

# 4 Model application and analysis of results

## 4.1 Experimental setup

In this section of the experiment, the main drive electromechanical system of a 350 mm experimental hot rolling mill is selected as the test object. The developed intelligent sensor is placed at the surface of the case of the main drive motor to collect the vibration, temperature, magnetic flux and noise parameters of the main drive motor. This paper describes the vibration signal as an example that can quickly react to the operating status of the main drive motor system. When the motor and its mill load failure occurs, there will be certain significant changes in the collected vibration signal, and the vibration signal is a relatively rapid change in the signal, by analyzing the vibration signal under various operating conditions helps to forecast the assessment of the operating status of the electromechanical system. Experimental test bearings through the EDM process set up a single point of failure, fault diameter were 0.007, 0.014, 0.021, 0.028 inches in four sizes. The experiments used accelerometers to collect vibration data from the motor drive end and the fan end, and the experimental data included four types of bearings under the operating conditions, namely, normal conditions, bearing wear, unbalance, and looseness.

When the diameter of the bearing failure is 0.007 inches and the motor load is 1 hp, the vibration signals under the four operating conditions are shown in Fig. 3 (Figs. a~d are normal operation, bearing wear, imbalance, and looseness, respectively). From the figure, it can be seen that the signal amplitude under normal state operation of the electromechanical system is fluctuating at 0V, while the signal amplitude under bearing wear, unbalance and looseness is fluctuating at -2~2V.

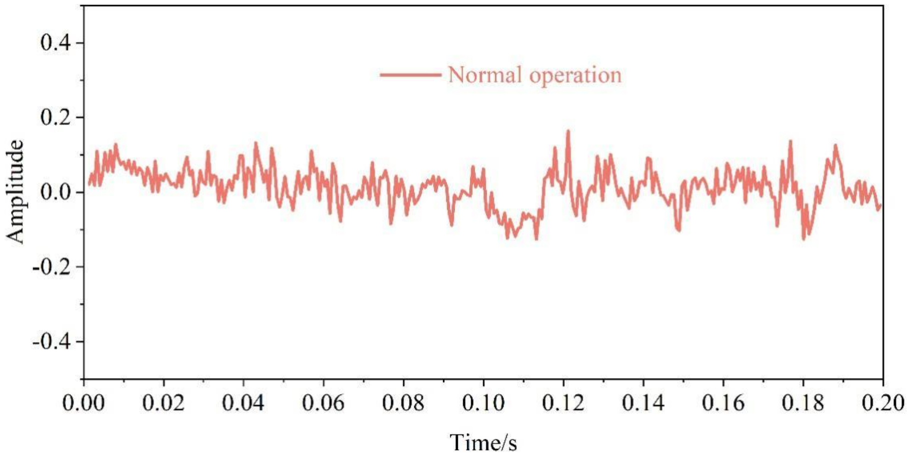


(a) Normal operation

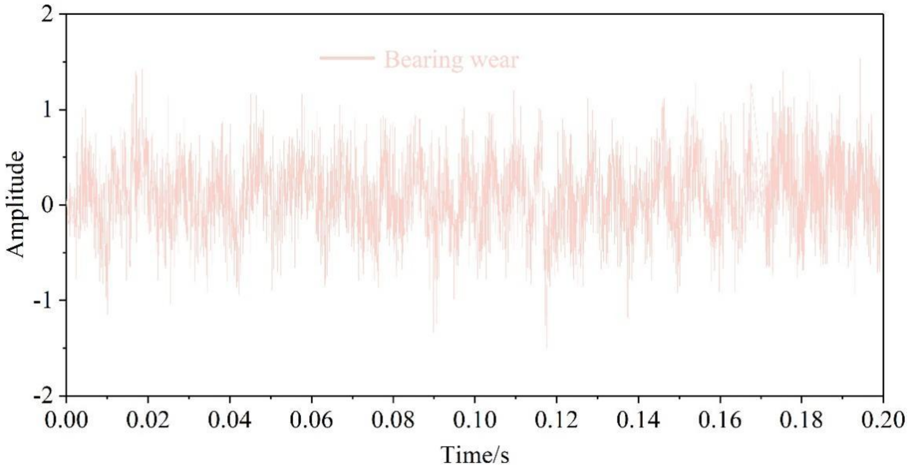


(b) Bearing wear

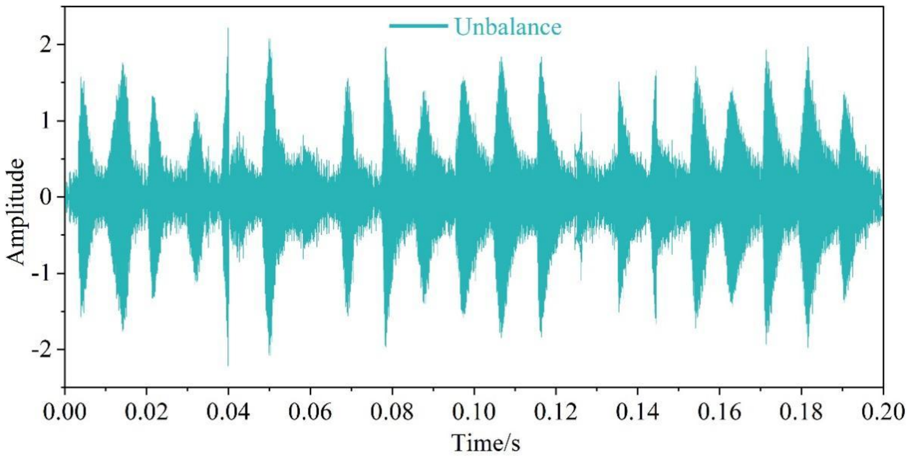


(c) Unbalance

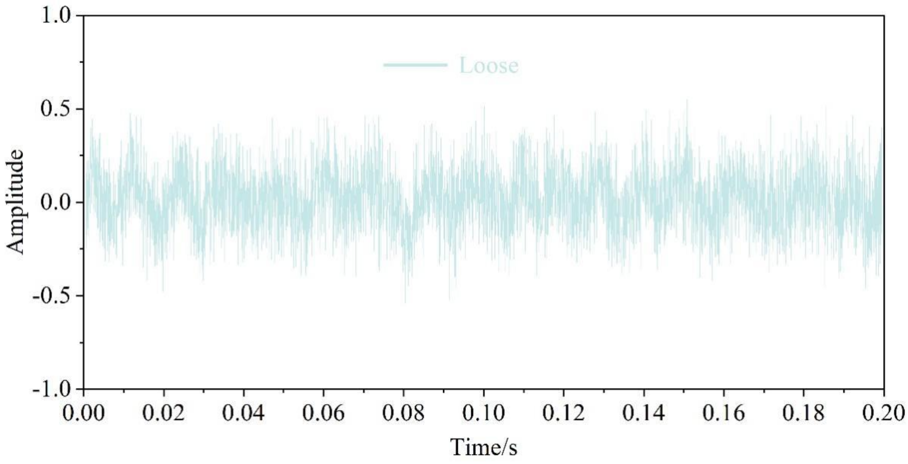


(d) Loose

*Figure 3: Vibration signal in four running states*

## 4.2 Electromechanical system vibration signal feature extraction and analysis

The features of the vibration signals in different states are extracted by time-frequency analysis methods, which mainly focus on the frequency features and time-domain features of the signals, including the peak vibration acceleration, spectral energy, frequency center, and root-mean-square value. Comparison of the spectrograms of different fault states is shown in Fig. 4, which clearly shows the changes in the position and amplitude of the characteristic frequencies of different fault states, and these features provide key support for the subsequent fault classification. The experimental results show that different fault modes present obvious characteristic differences within a specific frequency bandwidth, which are analyzed as follows.

(1) Bearing wear: A significant peak occurs at 50 Hz, reflecting the high-frequency vibration characteristics caused by bearing wear.

(2) Unbalanced state: the vibration signal has a significant increase in spectral energy in the rate interval from 14 Hz to 50 Hz, and the amplitude peak value increases significantly.

(3) Looseness: A strong energy distribution occurs in the low-frequency band of the signal (<20 Hz), indicating that the low-frequency vibration triggered by looseness is significant.

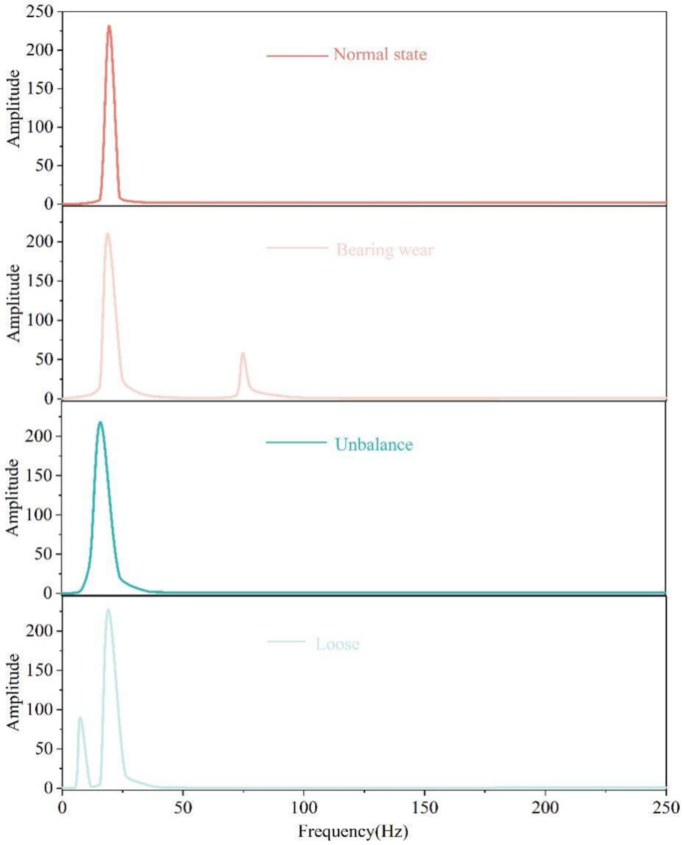


*Figure 4: The spectrum of different fault states is compared*

The vibration signal is analyzed by wavelet packet energy analysis, using demy wave to decompose the signal in 3 layers, to find the energy corresponding to all nodes in the 3 layers, and to select the energy of the first 4 nodes with obvious features as the feature vectors, which are recorded as $T_1$, $T_2$, $T_3$, and $T_4$, respectively. Ensuring that the other operating state parameters are the same, the feature vectors are extracted according to the above method for the vibration signals when the motor bearings are worn, unbalanced and loosened abnormally, respectively. The motor vibration eigenvectors under various states are shown in Table 2.

*Table 2: The vibration eigenvector of the motor under various conditions*

| Motor state | $T_1$ | $T_2$ | $T_3$ | $T_4$ |
|---|---|---|---|---|
| Normal operation | 6.3818 | 5.9268 | 0.0438 | 2.2229 |
| | 5.8674 | 5.49 | 0.0821 | 1.5681 |
| | 7.1524 | 4.3596 | 0.0726 | 1.593 |
| Bearing wear | 14.4918 | 30.6425 | 90.0325 | 3.6725 |
| | 11.9592 | 28.3971 | 95.1148 | 12.8257 |
| | 12.4078 | 34.3259 | 101.2178 | 14.6136 |
| Unbalance | 3.6656 | 9.2273 | 232.5878 | 4.6038 |
| | 4.42 | 3.8653 | 310.8037 | 2.4612 |
| | 3.9111 | 9.2228 | 320.9372 | 2.9655 |
| Loose | 2.2971 | 1.5474 | 11.5255 | 0.4109 |
| | 1.7488 | 1.9173 | 14.3668 | 0.1781 |
| | 2.2836 | 1.4674 | 16.1768 | 0.4404 |

The model in this paper is used to classify the vibration signals so as to realize the identification of the motor operating state. The vibration signals of the motor in four different operating states are collected, the vibration signals in different operating states are decomposed using wavelet packets, and the energy data of the first four wavelet nodes with obvious features are extracted from the third and used as the input sample data, and the operating state of the motor corresponding to the input sample data is used as the output sample data of the BP network. The number of nodes in the input layer is 4, the number of nodes in the output layer is 4, and the number of nodes in the hidden layer is 9 according to the corresponding rule, and the target data of the output is [1,0,0,0] when the motor is running normally, [0,1,0,0] when the inner ring is abnormal, [0,0,1,0] when the outer ring is abnormal, and [0,0,0,1] when the ball is abnormal. Randomly select 200 sets of sample data under different operating states for model training, and randomly select 20 sets of sample data to be used as test sets for motor operating state identification. After substituting the test set into the model, the recognition results are shown in Table 3. From the recognition results in the table and the test results of the 20 sets of test samples, it can be seen that the model in this paper can correctly recognize the running state of the motor with a high accuracy rate. For example, the average values of output 1~output 4 of the loose motor are 0.1829, 0.05097, 0.1476 and 0.7091, respectively, and its recognition result is a loose obstacle.

*Table 3: Identification result*

| Motor state | Output 1 | Output 2 | Output 3 | Output 4 | Identification result |
|---|---|---|---|---|---|
| Normal operation | 0.6068 | 0.0493 | 0.0239 | 0.3414 | Normal operation |
| | 0.82 | 0.0746 | 0.1484 | 0.3178 | Normal operation |
| | 1.1743 | 0.0518 | 0.0385 | 0.1046 | Normal operation |
| Bearing wear | 0.2514 | 0.8223 | 0.0646 | 0.118 | Inner loop anomaly |
| | 0.3406 | 1.1802 | 0.3372 | 0.1471 | Inner loop anomaly |
| | 0.1419 | 1.1657 | 0.0848 | 0.0922 | Inner loop anomaly |
| Unbalance | 0.0675 | 0.1037 | 1.0371 | 0.0287 | Exogynoanomaly |
| | 0.074 | 0.0697 | 0.997 | 0.3023 | Exogynoanomaly |
| | 0.141 | 0.0756 | 1.0863 | 0.2047 | Exogynoanomaly |
| Loose | 0.2989 | 0.0418 | 0.2969 | 0.6495 | Ball anomaly |
| | 0.231 | 0.0293 | 0.1321 | 0.7077 | Ball anomaly |
| | 0.0188 | 0.0818 | 0.0138 | 0.7701 | Ball anomaly |

The vibration signals of the main drive system of the experimental hot rolling mill are collected using the developed intelligent sensors, and the vibration signals of the normal operation of the experimental hot rolling mill are shown in Fig. 5.

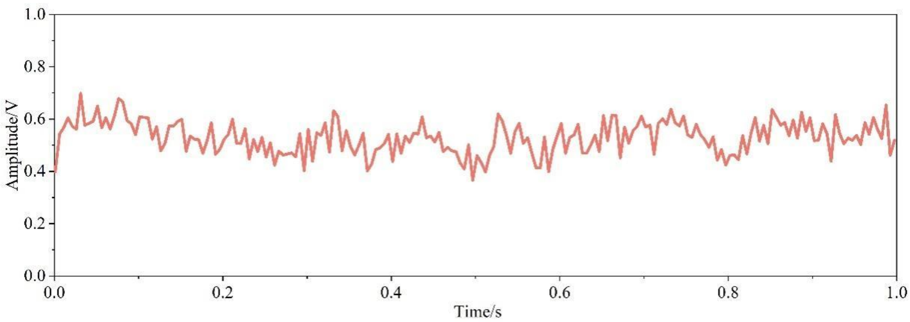


*Figure 5: Mechanical and electrical normal running vibration signal*

The normal operation vibration signal of the experimental hot rolling mill is feature extracted by the above method and substituted into the trained model, which yields the partial results of the mill operation state recognition as shown in Table 4. From the table of the mill running state part of the recognition results can be seen, output 1 ~ output 4 of the average value of 0.8683, 0.07268, 0.01704 and 0.08098. Trained in this paper's model can be better to identify the experimental mill's normal running state.

*Table 4: Run the status recognition part*

| state | Output 1 | Output 2 | Output 3 | Output 4 | Identification result |
|---|---|---|---|---|---|
| Normal operation | 0.891 | 0.0681 | 0.0195 | 0.062 | Normal operation |
| | 0.8647 | 0.0707 | 0.0083 | 0.0817 | Normal operation |
| | 0.8361 | 0.0575 | 0.0121 | 0.1222 | Normal operation |
| | 0.8661 | 0.0798 | 0.0129 | 0.0665 | Normal operation |
| | 0.8836 | 0.0873 | 0.0324 | 0.0725 | Normal operation |

# 5 Conclusion

Based on machine learning, the article realizes real-time monitoring of typical fault diagnosis of electric motors by preprocessing the signals and extracting the eigenvalues of motor operation vibration. The article draws the following conclusions:

When the electromechanical system is in an unbalanced state, the spectral energy of the vibration signal increases significantly in the rate interval from 14 Hz to 50 Hz, while the amplitude peak increases.

In the test results of 20 sets of test samples, the average values of output 1 to output 4 of the motor are 0.1829, 0.05097, 0.1476 and 0.7091, respectively.

In summary, the electromechanical system fault identification model designed by combining feature extraction and PSO-SVM in this paper can better identify the normal operation state of electromechanical system and has certain practical value.

# About the Author

Zhangwei Lei was born in Yuncheng, Shanxi. China, in 1981. He obtained a master's degree from Taiyuan University of Technology in China. He is currently working at Mechanical and Electrical Engineering Department, Yuncheng University. His main research direction is Automatic Control Technology and Intelligent Control.

# References

[1] Ballard, Z., Brown, C., Madni, A. M., & Ozcan, A. (2021). Machine learning and computation-enabled intelligent sensor design. Nature Machine Intelligence, 3(7), 556-565.

[2] Chang, F. C., & Huang, H. C. (2016). A Survey on Intelligent Sensor Network and Its Applications. J. Netw. Intell., 1(1), 1-15.

[3] Sharma, A., Sharma, V., Jaiswal, M., Wang, H. C., Jayakody, D. N. K., Basnayaka, C. M. W., & Muthanna, A. (2022). Recent trends in AI-based intelligent sensing. Electronics,

11(10), 1661.

[4] Liu, D. (2024, January). Application of electromechanical control system based on artificial intelligence control technology. In Proceedings of the 2024 International Conference on Power Electronics and Artificial Intelligence (pp. 934-938).

[5] Park, M., Bok, B. G., Ahn, J. H., & Kim, M. S. (2018). Recent advances in tactile sensing technology. Micromachines, 9(7), 321.

[6] Vo, T. S., & Kim, K. (2024). Recent Trends of functional composites and structures for electromechanical sensors: A review. Advanced Intelligent Systems, 6(5), 2300730.

[7] Fu, B., Damer, N., Kirchbuchner, F., & Kuijper, A. (2020). Sensing technology for human activity recognition: A comprehensive survey. Ieee Access, 8, 83791-83820.

[8] Pech, M., Vrchota, J., & Bednář, J. (2021). Predictive maintenance and intelligent sensors in smart factory. Sensors, 21(4), 1470.

[9] Nong, H., Jin, M., Pan, C., Zhou, H., Zhang, C., Pan, X., ... & Zhang, Z. (2024). Intelligent sensing technologies based on flexible wearable sensors: A review. IEEE Sensors Journal.

[10] Kumar, A., Singh, A., Kumar, A., Singh, M. K., Mahanta, P., & Mukhopadhyay, S. C. (2018). Sensing technologies for monitoring intelligent buildings: A review. IEEE Sensors Journal, 18(12), 4847-4860.

[11] Chen, Z., Fan, K., Wang, S., Duan, L., Lin, W., & Kot, A. C. (2019). Toward intelligent sensing: Intermediate deep feature compression. IEEE Transactions on Image Processing, 29, 2230-2243.

[12] Akhter, F., Khadivizand, S., Siddiquei, H. R., Alahi, M. E. E., & Mukhopadhyay, S. (2019). IoT enabled intelligent sensor node for smart city: pedestrian counting and ambient monitoring. Sensors, 19(15), 3374.

[13] Lakhiar, I. A., Jianmin, G., Syed, T. N., Chandio, F. A., Buttar, N. A., & Qureshi, W. A. (2018). Monitoring and control systems in agriculture using intelligent sensor techniques: A review of the aeroponic system. Journal of sensors, 2018(1), 8672769.

[14] Zhu, Y., Wang, M., Yin, X., Zhang, J., Meijering, E., & Hu, J. (2022). Deep learning in diverse intelligent sensor based systems. Sensors, 23(1), 62.

[15] Chen, X. (2023). Application of intelligent control in mechatronics system. Engineering Advances, 3(2).

[16] Jena, S., & Gupta, A. (2021). Review on pressure sensors: A perspective from mechanical to micro-electro-mechanical systems. Sensor Review, 41(3), 320-329.

[17] Ohalete, N., Aderibigbe, A., Ani, E., Ohenhen, P., & Daraojimba, D. (2024). Challenges and innovations in electro-mechanical system integration: A review. Acta Electronica Malaysia (AEM).

[18] Moon, F. C. (2017). Modeling Electromechanical Systems. Mechatronic Systems,

Sensors, and Actuators: Fundamentals and Modeling.

[19] Orhan, E., Yuksel, M., Ari, A. B., Yanik, C., Hatipoglu, U., Yağci, A. M., & Hanay, M. S. (2020). Performance of nano-electromechanical systems as nanoparticle position sensors. Frontiers in Mechanical Engineering, 6, 37.

[20] Coito, T., Firme, B., Martins, M. S., Vieira, S. M., Figueiredo, J., & Sousa, J. M. (2021). Intelligent sensors for real-Time decision-making. Automation, 2(2), 62-82.

[21] Wang, C., Dong, L., Peng, D., & Pan, C. (2019). Tactile sensors for advanced intelligent systems. Advanced Intelligent Systems, 1(8), 1900090.

[22] Aderibigbe, A. O., Ohenhen, P. E., Nwaobia, N. K., Gidiagba, J. O., & Ani, E. C. (2023). Advanced sensing techniques in electro-mechanical systems: surveying the rise of smart sensors and their implications for system robustness. Engineering Science & Technology Journal, 4(6), 323-340.

[23] Moon, J., & Leeb, S. B. (2018). Wire less sensors for electromechanical systems diagnostics. IEEE Transactions on Instrumentation and Measurement, 67(9), 2235-2246.

[24] Wang, S., Liu, S., Su, Z., Liu, L., & Tang, Z. (2024). Self-Sensing Electromechanical System Integrated with the Embedded Displacement Sensor. Sensors, 24(13), 4102.

[25] Nazir, S., & Kwon, O. S. (2022). Micro-electromechanical systems-based sensors and their applications. Applied Science and Convergence Technology, 31(2), 40-45.

[26] Esashi, M. (2012). Revolution of sensors in micro-electromechanical systems. Japanese journal of applied physics, 51(8R), 080001.

[27] Faudzi, A. A. M., Sabzehmeidani, Y., & Suzumori, K. (2020). Application of micro-electro-mechanical systems (MEMS) as sensors: A review. Journal of Robotics and Mechatronics, 32(2), 281-288.

[28] Zhou, G. (2021, July). Group Intelligence Perception Applied in the Electromechanical Equipment Fault Intelligent Diagnosis Support System. In Journal of Physics: Conference Series (Vol. 1982, No. 1, p. 012054). IOP Publishing.

[29] Lingli Yao. (2025). Research on the application of intelligent sensors based on the Internet of Things in fault diagnosis of mechanical and electrical equipment. Measurement: Sensors,38,101811-101811.

[30] Vikash Kumar Singh,Kalpana Sharma & Samarendra Nath Sur. (2025). Impact of various continuous wavelet transforms for acoustic scene classification with DCASE dataset. Signal, Image and Video Processing,19(6),440-440.

[31] National Institute of Technology, Goa,National Institute of Technology, Goa,Madanapalle Institute of Technology and Science & National Institute of Technology, Goa. (2019). An efficient Concealed Information Test: EEG feature extraction and ensemble classification for lie identification. Machine Vision and Applications,30(5),813-832.

[32] Baranwal Anubhav,Gaurav Prince,Reddy Lohit,Das Bhabani Shankar & Naik Balaji.

(2024). Predicting temporal clear water scour depth around bridge piers with XGBoost and SVM–PSO approaches. Journal of Hydroinformatics,26(12),3109-3129.